Title

Minireview - Microtubules and Tubulin Oligomers: Shape Transitions and Assembly by Intrinsically Disordered Protein Tau and Cationic Biomolecules.

Journal

Langmuir, 35(48)

Authors

Safinya, Cyrus

Chung, Peter

Song, Chaeyeon

et al.

Publication Date

2019-12-03

DOI

10.1021/acs.langmuir.9b02208

Peer reviewed

Published in final edited form as:

Langmuir. 2019 December 03; 35(48): 15970–15978. doi:10.1021/acs.langmuir.9b02208.

Minireview - Microtubule and Tubulin Oligomers: Shape Transitions and Assembly by Intrinsically Disordered Protein Tau and Cationic Biomolecules

Cyrus R. Safinya[1,*], **Peter J. Chung**[2], **Chaeyeon Song**[3], **Youli Li**[4], **Herbert P. Miller**[5], **Myung Chul Choi**[6], **Uri Raviv**[7], **Kai K. Ewert**[1], **Leslie Wilson**[5], **Stuart C. Feinstein**[5]

[1]Materials Department, Physics Department, Molecular, Cellular, and Developmental Biology Department, University of California, Santa Barbara, California 93106, USA

[2]James Franck Institute and Department of Chemistry, University of Chicago, Illinois 60637, USA

[3]Amorepacific Corporation R&D Center, Yongin 17074, Republic of Korea

[4]Materials Research Laboratory, University of California, Santa Barbara, California 93106, USA

[5]Neuroscience Research Institute and Molecular, Cellular, and Developmental Biology Department, University of California, Santa Barbara, California 93106, USA

[6]Department of Bio and Brain Engineering, Korea Advanced Institute of Science and Technology (KAIST), Daejeon 305-701, Republic of Korea

[7]Institute of Chemistry and the Center for Nanoscience and Nanotechnology, The Hebrew University of Jerusalem, Edmond J. Safra Campus, Givat Ram, Jerusalem 9190401, Israel

Abstract

In this mini-review, which is part of a special issue in honor of Jacob N. Israelachvili's remarkable research career on intermolecular forces and interfacial science, we present studies of structures, phase behavior, and forces in reaction mixtures of microtubules (MTs) and tubulin oligomers, with either intrinsically disordered protein (IDP) Tau, cationic vesicles, or the polyamine spermine (4+). Bare MTs consist of thirteen protofilaments (PFs) on average where each PF is made of a linear stack of αβ-tubulin dimers (i.e. tubulin oligomers). We begin with a series of experiments, which demonstrate the flexibility of PFs towards shape changes in response to local environmental cues. First, studies show that MT-associated protein (MAP) Tau controls the diameter of microtubules upon binding to the outer surface implying a shape change in the cross-sectional area of PFs forming the MT perimeter. The diameter of a MT may also be controlled by the charge

*Corresponding author: safinya@mrl.ucsb.edu.

density of a lipid bilayer membrane that coats the outer surface. We further describe an experimental study where it is unexpectedly found that the biologically relevant polyamine spermine (+4e) is able to depolymerize *taxol-stabilized* microtubules with efficiency that increases with decreasing temperature. This MT destabilization drives a dynamical structural transition where inside-out curving of PFs, during the depolymerization peeling process, is followed by re-assembly of ring-like curved PF building blocks into an array of helical inverted tubulin tubules. We finally turn to a very recent study on pressure-distance measurements in bundles of MTs employing the small-angle X-ray scattering (SAXS)-osmotic pressure technique, which complements the Surface-Forces Apparatus technique developed by Jacob N. Israelachvili. These latter studies are among the very few, which are beginning to shed light on the precise nature of the interactions between MTs mediated by MAP Tau in 37°C reaction mixtures containing GTP and lacking taxol.

Graphical Abstract

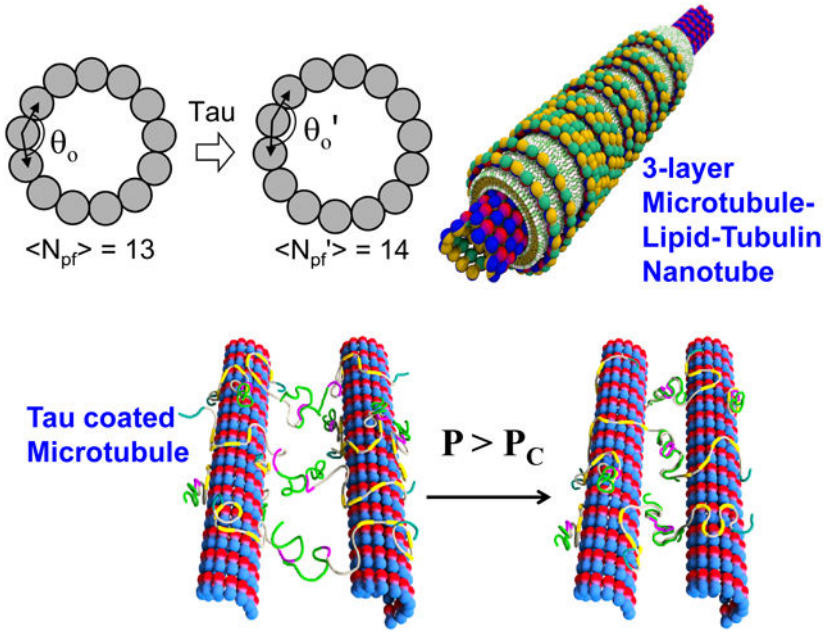

Keywords

Intrinsically disordered protein Tau; cytoskeletal filaments; tubulin and microtubules; microtubule-associate protein; force measurements with SAXS-osmotic pressure

INTRODUCTION

One of the many objectives in biophysics is to elucidate the nature of interactions between biological macromolecules including, for example, proteins, nucleic acids, lipids, which are responsible for the assembly of these building blocks on length scales from nanometers to microns of the order the cell size. This is because the various assembled structures and, in particular, the exposed surface shapes are often important to distinct cell functions. For example, during the cell cycle, extensive remodeling of cytoskeletal protein assemblies

enables the complex process of cell division.[1] This mini-review is, in part, focused on the long-term goal to develop a comprehensive understanding of structures and forces between reconstituted cytoskeletal filamentous microtubules (MTs) and associated proteins, in particular, those derived or purified from neurons. We expect that such an understanding will address the key question of how the physical properties of cytoskeletal assemblies impact neuronal cell functions.[2,3]

To begin our discussion of the cytoskeleton of neurons we show in Fig. 1A a drawing of a neuron where key subcellular components of the axon, cell body, and dendrites are depicted.[4] This cartoon is accompanied by high-resolution quick-freeze and deep-etched electron micrographs by Nobutaka Hirokawa and collaborators displaying the highly distinct cytoskeletons of the axon and dendrite of vertebrate neurons with a large fraction of the intracellular space occupied by MTs and neurofilaments (NFs) (Fig. 1 (B,C)).[5,6] Microtubules are the dominant filaments in dendrites and are normally distributed throughout the cytoskeleton as single filaments (see Fig. 1B where one of the MTs is labeled with a yellow star). Neurofilaments (NFs, Fig. 1B, white arrow points to one NF) are either singly dispersed between MTs or appear in small bundles (Fig. 1B, labeled by a red star).[3,5] In contrast, in axons, NFs, which are oriented parallel to the axon, constitute the major cytoskeletal filaments (Fig.1C, red stars show the extensive NF-network). NFs, the intermediate filaments of neurons, consist of a core cylindrical body (≈ 10 nm diameter, Fig. 1C, white arrow) with protruding charged sidearms (Fig. 1C, yellow arrow) cross-linking neighboring filaments into a network.[3,6] When NF networks are reconstituted from purified NF-subunits they consist of liquid crystalline hydrogels under physiological pH and salt conditions.[7–10] MTs, which are immersed within the extended NF-network in axons, are primarily found to be isolated along the long axon. The exception to this is in the axon initial-segment (Fig.1A) where MTs are found to form small linear bundles commonly referred to as MT fascicles (Fig. 1C, blue star).[11] Interestingly, linear MT fascicles are also found to form spontaneously outside cells in reaction mixtures of tubulin and MAP Tau at 37°C in the presence of buffer containing GTP and 1mM of Mg^{2+}.[12]

In non-dividing mature neurons, members of microtubule-associated proteins (MAPs) bind to and stabilize MTs against depolymerization. MAP Tau and MAP2 stabilize MTs in axons and dendrites, respectively.[13–19] EM studies show that MAPs may cross-bridge MTs into bundles in axons (Fig. 1C, red arrow).[5,6] Furthermore, NF-sidearms have been implicated in cross-linking NFs to MTs in axons (Fig. 1C, blue arrow). The electron micrographs of Fig. 1, depicting co-existence of MTs and NFs, highlight the formation of the distinct cytoskeletal structures present in axons and dendrites.

MAP Tau is an intrinsically disordered protein (IDP) and a biological polyampholyte (i.e. a charged polymer containing both positive and negative charged groups, see Fig. 2). Similarly, the C-terminal sidearms of NFs are intrinsically disordered polyampholytes projecting radially away form the NF cylindrical core.[7–10] While complementary protein shapes mediate induced-fit lock-and-key interactions in folded proteins,[1] IDPs play an important, yet poorly understood role, in mediating non-specific interactions.[20–22]

The review is organized as follows. We first describe experiments on mixtures of taxol-stabilized MTs and MAP Tau isoforms as a function of increasing Tau/tubulin dimer molar ratio (i.e. increases in the coverage of the MT surface with Tau).[23] Here, we find that MAP Tau modifies the average number of PFs in MTs thus modifying the MT diameter. Remarkably, experiments also show that the MT diameter may also be varied by changes in the charge density of an adhering cationic lipid bilayer coating the outer surface of the MT.[24,25] The two studies demonstrate how attractive electrostatic interactions, whether it is between microtubules and Tau's cationic microtubule binding regions or cationic liposomes, alter the cross-sectional area of PFs forming the perimeter of MTs. We next turn to a brief review of recent studies of the effect of polyamine spermine (4+), a multivalent counterion to anionic MTs, on the assembly structure of MTs.[26] At short times, spermine induces MT bundling.[27] However, with increasing time, spermine has a destabilizing effect on MTs by rupturing ionic bonds between PFs that make up the curved surface of MTs. The depolymerization of MTs via peeling of PFs leads to PF ring formation, which, in turn, leads to the stacking of PF-rings into helical inverted tubulin tubules. The tubules are referred to as inverted because the outer surface corresponds to the inner surface of MTs. These cell-free studies, which showed how multivalent spermine influences the overall stability of MT bundles are highly significant in elucidating how biologically related small biomolecules may play a fundamental role in modulating and remodeling the cytoskeleton in vivo, an emerging field of very high current interest in biological physics.

In the last part of the review we turn to recent studies, which demonstrate how the synchrotron SAXS-osmotic pressure technique allows one to obtain pressure-interfilament distance curves in dissipative reaction mixtures of tubulin and Tau at 37° C in the presence of the fuel molecule GTP required to maintain the dynamical bundled structure.[28] The technique was introduced in the biophysics community by Adrian Parsegian and collaborators over many years,[29] It complements the surface-forces-apparatus (SFA) methodology developed by Jacob Israelachvili for measuring forces between surfaces coated with a wide variety of macromolecules.[30.] This more recent study also shows how forces between microtubules are fundamentally altered when comparisons are made between taxol-stabilized microtubules, described in the first part of the review, and microtubules undergoing dynamic instability with cycles of growth and shortening due to GTP hydrolysis.

MICROTUBULE-ASSOCIATED PROTEIN TAU REGULATES THE NUMBER OF PROTOFILAMENTS IN MICROTUBULES

Microtubules (MTs) are hollow cylinders with outer and inner diameters of about 25 nm and 15 nm, respectively (Fig. 2A).[31–35] Their building blocks are αβ-tubulin heterodimers (red/blue spheres in Fig. 2A), which stack to form linear protofilaments (PFs). During tubulin assembly, lateral interactions between tubulin oligomers (PFs of various lengths) leads to the curved MT wall. MTs are inherently dynamical and exhibit alternating periods of growth (tubulin polymerization) and shrinkage (depolymerization events or catastrophes) referred to as dynamic instability.[31,32] MTs and their dynamical assemblies are utilized by cells, typically in combination with MAPs, for a variety of activities, including, intracellular trafficking and chromosome segregation.[33,34]

Human MAP Tau consists of six isoforms (Fig. 2B), those containing four C-terminal imperfect repeats, constituting the cationic MT binding domains R1–R4 and labeled 4R-Tau (see cartoon of Tau bound to MT in Fig. 2A), and those with three repeats (3R-Tau, R1–R3). Each family contains three distinct alternatively spliced isoforms, yielding N-terminal short (S), medium (M), and long (L) projection domains. The six Tau isoforms are labeled: 4RS, 4RM, 4RL, 3RS, 3RM, and 3RL, respectively. The N-terminal tail (NTT) consists of an anionic/cationic dipolar projection domain (PD) that projects off the MT surface, followed by a cationic proline rich domain with some MT affinity (Fig. 2B). The carboxyl-terminal tail (CTT) has low MT affinity.

The binding of different isoforms of Tau through the cationic binding domains (labeled MTBR, Fig. 2B) to MTs that are overall negative with charge density $\approx -0.66e/nm^2$, stabilizes MTs against dynamic instability.[36–40] Aberrant behavior in Tau is responsible for neurodegenerative diseases including Alzheimer's disease, Fronto-Temporal Dementia with Parkinsonism linked to chromosome-17, and Chronic Traumatic Encephalopathy in athletes.[41–43]

In a recent study by Choi et al.[23] the cancer chemotherapy drug paclitaxel, which is referred to as taxol in the tubulin community, was used to fix microtubules against dynamic instability.[44–49] Synchrotron small-angle X-ray scattering (SAXS) was used to probe the structure of taxol-stabilized MTs in the presence of the human MAP Tau isoforms. The study revealed that Tau isoforms regulate the average size of the diameter of MTs at the ångstrom scale.[23] An example of the SAXS scattering profile for the 4RS-Tau isoform is shown in Figure 3A. The data corresponds to the form factor of MTs that was modeled as a hollow cylinder with the inner radius $<R_{in}^{MT}>$ being the fitting parameter at constant wall thickness $\delta_w = 49$ Å consistent with high resolution electron microscopy models of MTs with 13 protofilaments.[49]

Most notably, the form factor SAXS data provide strong evidence that MAP Tau regulates the distribution of protofilament numbers in MTs. This is seen in the shift of the first minimum in SAXS, which is inversely proportional to the diameter of MTs, to lower q values as Φ (the tau to tubulin-dimer molar ratio in the reaction mixture) increases. Figure 3B is a plot depicting the increase of the average inner wall radius $<R_{in}>$ of MTs and, equivalently, the corresponding average number of PFs per MT, $<N_{pf}>$, with increasing ϕ (the tau to tubulin-dimer molar ratio for the fraction of Tau bound to the MT surface). Significantly, $<R_{in}>$ was observed to increase for $0 < \phi < 0.2$ and saturate for ϕ between 0.2 and 0.5. Thus, the data show that a local shape distortion of the tubulin dimer upon tau binding, is spread collectively over many dimers along the length of protofilament. The findings imply that MAP Tau mediates changes in the cross-sectional area of PFs forming the perimeter of MTs. This change in PF shape will result in changes in the number of PFs in MTs and thus the MT diameter.

Our findings imply that MAP Tau regulates the shape of *individual* protofilaments because it binds to only one side of the protofilament facing outwards away from the luminal surface of the MT. This will then change the spontaneous curvature of microtubules leading to changes in the measured curvature, which is inversely proportional to the MT radius. An important

biological implication of these findings is a possible allosteric role for MAP Tau where the induced shape changes of the MT surface upon binding by tau may affect the MT binding activity of other MAPs present in neurons. Furthermore, the results, which provide insight on the regulation of the elastic properties of MTs by MAP Tau, due to changes in the MT diameter, may also have relevance to the mechanical properties of the cell cytoskeleton.

Stepwise Nanometer-Scale Changes in the Diameter of Microtubules Driven by a Cationic Lipid Bilayer Coating.

In an earlier study Raviv et al. investigated the interactions between cationic lipid vesicles and Microtubules and discovered that the mixture results in the spontaneous formation of lipid protein nanotubules (LPNs) under the appropriate conditions (Fig. 4A,B).[24,25] The LPNs exhibit a remarkable architecture with the lipid bilayer sandwiched between the microtubule and an outer tubulin oligomer layer.

The degree of overcharging of the lipid-protein nanotube enables the switching between two states of the LPN with either closed ends with lipid caps (when the LPN is positively overcharged) or open ends seen in Fig. 4A, when the LPN is negatively overcharged. This would form the basis for controlled chemical encapsulation and release.[24] Raviv et al. further discovered that the average number of protofilaments in MTs may be controlled by changes in the membrane charge density of the lipid bilayer coating the MT.[25] Figure 4C shows that as the membrane charge density, proportional to the molar fraction of cationic lipid x_{CL}, increases, the average number of protofilaments per microtubule ($<N_{pf}>$) and thus the inner radius $<R_{in}>$, decreases. What is surprising is that the change occurs in a step-wise fashion. Thus, the inner and outer diameters of the lipid-protein nanotube - a key parameter in chemical encapsulation and templating applications - may be controlled and varied by changes in the membrane charge density of the enveloping cylindrical lipid bilayer.

TRANSFORMATION OF TAXOL-STABILIZED MICROTUBULES INTO INVERTED TUBULIN TUBULES TRIGGERED BY A TUBULIN CONFORMATION SWITCH

A recent study by Ojeda-Lopez et al. employed the shape changing property of protofilaments, resulting from the enzymatic properties of the αβ-tubulin heterodimers, to study the impact on new self assembling structures.[26] The study took advantage of the well known property of PFs to exist in either a straight or curved conformation with the transition between these two states controlled by GTP hydrolysis.[31–35] The distinct conformations of PFs underlie the broad range of cellular activities of tubulin and polymerized tubulin (i.e. microtubules), which include imparting cell shape, as tracks for organelle transport, and as building blocks of dynamical spindles.[1] The work by Ojeda-Lopez et al. led to the remarkable discovery that tetravalent spermine (4+) controls the straight to curved transition rate even in *taxol-stabilized* tubulin.[26,50] This led to the creation of microtubule bundles in the presence of spermine on short time scales (Fig. 5B), which at longer times, undergo a dynamical transformation involving an inside-out curving of tubulin oligomers during the depolymerization peeling process (Fig. 5C) and concurrent re-assembly of curved tubulin building blocks into an array of inverted tubulin tubules (Fig. 5D). This new phase of tubulin

assembly has been defined as a phase of bundles of inverted tubulin tubules (B_{ITT}). Thus, the study[26] led to a revision of the dogma in the MT field[50] that taxol-stabilized MTs were stable over extended periods of order months.

INTERFILAMENT FORCES IN MICROTUBULES BUNDLED BY TAU BY THE SAXS-OSMOTIC PRESSURE TECHNIQUE

The forces between filamentous MTs may be measured by using the SAXS-osmotic pressure technique, which involves performing in situ SAXS measurements of samples under osmotic pressure induced by a water soluble polymer depletant; for example, poly(ethylene oxide, PEO).[28,29,51,52] Synchrotron SAXS and TEM by Chung et al. show that dynamical MT bundles form spontaneously in reaction mixtures of Tau, tubulin, and GTP at 37°C (i.e. under dissipative conditions similar to the intracellular environment).[12] TEM of such bundles are depicted in Fig. 6A and synchrotron SAXS measurements reveal a wide wall-to-wall spacings ($D_{w–w}$) similar to that of MT bundles found in the axon initial-segment (see Fig. 1A,C). For example, for the 3RS Tau isoform, $D_{w–w} \approx 27$ nm (Fig. 6B, at zero osmotic pressure).

Figure 6B (magenta colored squares) displays the osmotic-pressure versus MT wall-to-wall spacing (P-D_{w-w}) curve for the 3RS-Tau isoform at a Tau/tubulin dimer molar ratio of 1/20 where D_{w-w} is obtained by synchrotron SAXS of MT/Tau bundles as a function of increasing wt% 102K-PEO (M_W = 100kDa).[28] The 102K-PEO is expected to have a diameter d100K-PEO = $4R_G/\pi^{1/2} \approx 40$ nm.[52] Here, $R_G = 0.215MW^{0.583}$ Å.[53] The relatively large size of 102K-PEO does not penetrate the interior region of the MT bundles and exerts an osmotic pressure on the bundle, which is a function of the concentration of the water soluble polymer.[28,51,53] Figure 6B shows that as a function of increasing wt% of 102K-PEO, the P-D_{w-w} curve exhibits a sharp rise between 40 Pa and ≈ 300 Pa and D_{w-w} decreases about 2 nm to 3 nm. The repulsive barrier is from Tau's projection domain resisting osmotic compression (see Fig. 2). Above a critical pressure $P > P_c \approx 300$ Pa, there is a rapid decrease in D_{w-w} from about 21.5 nm to 16.5 nm signaling a collapse of the bundle.

The large MT wall-to-wall spacing $D_{w-w} \approx 27$ nm measured by SAXS for MTs bundled by 4RS Tau at P = 0 results from an extended state for Tau's projection domain (PD). In this state the MT/Tau bundles are stabilized by attractions between oppositely charged residues of weakly penetrating apposing PDs between neighboring MT (Fig. 6C). The sudden transition above P_c indicates the onset of attraction between interpenetrating Tau chains on opposing MT surfaces, which would result in the decrease in D_{w-w} from ≈ 21.5 nm to ≈ 16.5 nm consistent with anti-parallel dimerization of Tau's PDs (Fig. 6D) (i.e. due to the dipolar charge distribution of the PD, Fig. 2C). MTs bundled by PD dimers are in a second local energy minimum with a smaller wall-to-wall spacing distinct from the minimum in widely-spaced bundles at P = 0.

Figure 6B also plots the PD curve with 20K-PEO (green squares), which is the most widely used depletant in SAXS-osmotic pressure studies.[29,51] The abrupt decrease in D_{w-w} with 20K-PEO is now observed at higher pressures ≈ 5000 Pa by about an order of magnitude. This is because 20K-PEO is able to partially penetrate the MT bundle region due to its

smaller diameter d20K-PEO (= $4R_G/\pi^{1/2}$) ≈ 15.6 nm less than $D_{w\text{-}w}$ ≈ 27 nm. This leads to a gradient in concentration of 20K-PEO between the outside and inside of the bundle effectively lowering the actual applied osmotic pressure. The “apparent pressure” plotted in Fig. 6B (green squares), which assumes all 20K-PEO is outside the bundle, is larger than the applied pressure (i.e. due to the difference in 20K-PEO concentration between outside and inside of the bundle) and so the transition to the collapsed MT bundle state is seen to occur at a higher “apparent pressure”. As expected we see that once the transition to the collapsed bundle state occurs the data for measurements with 20K-PEO and 100K-PEO are in agreement. This is because at the smaller spacings ≈ 5.0–6.0 nm, less than the diameter of 20K-PEO, 15.6 nm, the polymer is expelled from the bundle interior.

SUMMARY

We have presented an overview of recent work on the structural transitions related to shape changes in protofilaments, which make up the wall of microtubules, in the presence of intrinsically disordered protein Tau and separately cationic vesicles. In addition, we reviewed a study, which revealed how tetravalent spermine (4+), a biologically relevant polyamine with multiple distinct functions in cells,[54] may direct an evolution in the structure of taxol-stabilized microtubules. While at short times spermine bundles microtubules, at longer times, it leads to depolymerization of taxol-stabilized microtubules and stacking of stable tubulin rings in a helical manner creating an inverted tubulin tubule. MT disassembly and tubulin re-assembly is also notable because the surface that is on the *inside* of the microtubules is switched to the *outside* on the new array of inverted tubulin tubules; thus, stably exposing the “inner lumen” of microtubules. This provides a unique platform for experiments addressing interactions of biomolecules, in particular, MT-associated proteins, with the inner surface of MTs.

The SAXS-osmotic pressure technique, which was used to measure interfilament forces between Tau-coated MTs is nearly unique among force measuring techniques in enabling quantitative force measurements between filaments in suitable buffer conditions (pH, salt concentrations) with *minimal disturbance* to the bulk hydrogel containing the cytoskeletal filaments. This technique yields similar information obtainable from the surface-forces-apparatus (SFA) invented by Jacob N. Israelachvili. Our demonstration that the SAXS-osmotic pressure technique may access both repulsive and attractive regimes, and, measure the mechanical stability of MT/Tau bundles, suggests the feasibility of this type of force measurements in future studies in co-assembling mixtures of MTs and neurofilaments. For example, such measurements would allow one to obtain, *for the first time*, direct information on interfilament forces in interacting mixtures of MT and neurofilament hydrogels mimicking the cytoskeleton of different neuronal compartments (axons, cell body, and dendrites) (see Fig. 1), and should be transformative in yielding fundamentally new insights connecting forces to heterogeneously assembled structures.

ACKNOWLEDGEMENTS

This work was supported by the US Department of Energy (DOE), Office of Basic Energy Sciences, Division of Materials Sciences and Engineering under award number DE-FG02-06ER46314 (self- and directed assembly in charged biomolecular materials systems). Partial support was further provided by the US National Science

Foundation (NSF) under award number DMR-1807327 (protein phase behavior) and the US National Institutes of Health under award numbers R01-NS13560 and R01-NS35010 (tubulin purification and protein Tau isoform purification from plasmid preparations). M.C.C. was supported by NRF 2017M2A2A6A01071190, NRF-2018R1A2B3001690, KC30 N11170021, KUSTAR-KAIST Institute, KAERI and APCTP. U.R. was support by the Israel Science Foundation (grant 656/17). The X-ray diffraction work was carried out at the Stanford Synchrotron Radiation Lightsource, a Directorate of SLAC National Accelerator Laboratory and an Office of Science User Facility operated for the US DOE Office of Science by Stanford University.

REFERENCES

(1). Alberts B; Johnson A; Lewis J; Raff M; Roberst K; Walter P: Molecular Biology of the Cell 4th ed., 2002, Garland Science, New York.

(2). Peters A; Palay SL; Def H: The Fine Structure of the Nervous System. 3rd ed., 1991, Webster, New York.

(3). Burgoyne RD (Ed.): The Neuronal Cytoskeleton. 1991, Wiley & Sons, New York.

(4). Brady S, Colman DR, Brophy P. Subcellular Organization of the Nervous System: Organelles and Their Functions (Chapter 4) In “Fundamental Neuroscience”, Eds. Zigmond MJ, Bloom FE, Landis SC, Roberts JL, Squire LR; 1999, Academic Press, New York.

(5). Hirokawa N; Hisanaga S-I; Shiomura Y: MAP2 is a Component of Crossbridges Between Microtubules and Neurofilaments in the Neuronal Cytoskeleton: Quick-Freeze, Deep-Etch lmmunoelectron Microscopy and Reconstitution Studies. J. Neurosci 1988, 8, 2769–2779. [PubMed: 3045269]

(6). Hirokawa N: Cross-Linker System between Neurofilaments, Microtubules, and Mem-branous Organelles in Frog Axons Revealed by the Quick-Freeze, Deep-Etching Method. J.Cell Biol 1982, 94, 129–142. [PubMed: 6181077]

(7). Jones JB; Safinya CR: Interplay between Liquid Crystalline and Isotropic Gels in Self-Assembled Neurofilament Networks. Biophys. J 2008, 95, 823–825. [PubMed: 18583309]

(8). Beck R; Deek J; Jones JB; Safinya CR: Gel Expanded–Gel Condensed Transition in Neurofilament Networks Revealed by Direct Force Measurements. Nature Materials 2010, 9, 40–46. [PubMed: 19915555]

(9). Deek J; Chung PJ; Kayser J; Bausch AR; Safinya CR: Neurofilament sidearms modulate parallel and crossed-filament orientations inducing nematic to isotropic and re-entrant birefringent hydrogels. Nature Communications 2013, 4, 2224.

(10). Deek J; Chung PJ; Safinya CR: Neurofilament networks: Salt-responsive hydrogels with sidearm-dependent phase behavior. Biochim. Biophys. Acta–General Subjects 2016, 1860, 1560–1569.

(11). Rasband MN: The axon initial segment and the maintenance of neuronal polarity. Nat. Rev. Neurosci 2010, 11, 552–562. [PubMed: 20631711]

(12). Chung PJ; Song C; Deek J; Miller HP; Li Y; Choi MC; Wilson L; Feinstein SC; Safinya CR: Tau mediates microtubule bundle architectures mimicking fascicles of microtubules found in the axon initial segment. Nature Commun. 2016, 7, 12278. [PubMed: 27452526]

(13). Kosik KS; Finch EA: MAP2 and tau segregate into dendritic and axonal domains after the elaboration of morphologically distinct neurites: An immunocytochemical study of cultured rat cerebrum. J. Neurosci 1987, 7, 3142–3153. [PubMed: 2444675]

(14). Hirokawa N; Funakoshi T; Sato-Harada R; Kanai Y: Selective stabilization of tau in axons and microtubule-associated-protein 2 in cell bodies and dendrites contributes to polarized localization of cytoskeletal proteins in mature neurons. J. Cell Biol 1996, 132, 667–679. [PubMed: 8647897]

(15). Caceres A; Kosik KS: Inhibition of neurite polarity by tau antisense oligonucleotides in primary cerebellar neurons. Nature 1990, 343, 461–463. [PubMed: 2105469]

(16). Esmaeli-Azad B; McCarty JH; Feinstein SC: Sense and antisense transfection analysis of tau function: tau influences net microtubule assembly, neurite outgrowth and neuritic stability. J. Cell Sci 1994, 107, 869–879. [PubMed: 8056843]

(17). Dawson HN; Ferreira A; Eyster MV; Ghoshal N; Binder LI; Vitek MP: Inhibition of neuronal maturation in primary hippocampal neurons from tau-deficient mice. J. Cell Sci 2001, 114, 1179–1187. [PubMed: 11228161]

(18). Harada A; Teng J; Takei Y; Oguchi K; Hirokawa N: MAP2 is required for dendrite elongation, PKA anchoring in dendrites, and proper PKA signal transduction. J. Cell Biol 2002, 158, 541–549. [PubMed: 12163474]

(19). Dehmelt L; Halpain S: The MAP2/Tau family of microtubule-associated proteins. Genome Biol. 2004, 6, 1–10.

(20). Dunker KA; Kriwacki RW: The orderly chaos of proteins. Sci. Am 2011, 304, 68–73. [PubMed: 21495485]

(21). Dyson HJ; Wright PE: Intrinsically unstructured proteins and their functions. Nature Rev. Cell Biol 2004, 6, 197–208.

(22). Tompa P: Intrinsically unstructured proteins. Trends Biochem. Sci 2002, 27, 527–533. [PubMed: 12368089]

(23). Choi MC; Raviv U; Miller HP; Gaylord MR; Kiris E; Ventimiglia D; Needleman DJ; Kim MW; Wilson L; Feinstein SC; Safinya CR: Human Microtubule-Associated-Protein Tau Regulates the Number of Protofilaments in Microtubules: A Synchrotron X-ray Scattering Study. Biophys. J 2009, 97, 519–527. [PubMed: 19619466]

(24). Raviv U; Needleman DJ; Li YL; Miller HP; Wilson L; Safinya CR: Cationic liposome–microtubule complexes: Pathways to the formation of two-state lipid–protein nanotubes with open or closed ends. Proc. Natl. Acad. Sci. U. S. A 2005, 102, 11167–11172. [PubMed: 16055561]

(25). Raviv U; Nguyen T; Ghafouri R; Needleman DJ; Li YL; Miller HP; Wilson L; Bruinsma RF; Safinya CR: Microtubule protofilament number is modulated in a stepwise fashion by the charge density of an enveloping layer. Biophys. J 2007, 92, 278–287. [PubMed: 17028134]

(26). Ojeda-Lopez MA; Needleman DJ; Song C; Ginsburg A; Kohl P; Li Y; Miller HP; Wilson L; Raviv U; Choi MC; Safinya CR: Transformation of taxol-stabilized microtubules into inverted tubulin tubules triggered by a tubulin conformation switch. Nature Materials 2014, 13, 195–203. [PubMed: 24441880]

(27). Needleman DJ; Ojeda-Lopez MA; Raviv U; Miller HP; Wilson L; Safinya CR: Higher-order assembly of microtubules by counterions: From hexagonal bundles to living necklaces. Proc. Natl. Acad. Sci. U. S. A 2004, 101, 16099–16103. [PubMed: 15534220]

(28). Chung PJ; Song C; Deek J; Miller HP; Li Y; Choi MC; Wilson L; Feinstein SC; Safinya CR: Comparison between 102k and 20k Poly(ethylene oxide) Depletants in Osmotic Pressure Measurements of Interfilament Forces in Cytoskeletal Systems. ACS Macro Lett. 2018, 7, 228–232.

(29). Parsegian VA; Rand RP; Fuller NL; Rau DC: Osmotic-stress for the direct measurement of intermolecular forces. Meth. Enzymol 1986, 127, 400–416. [PubMed: 3736427]

(30). Israelachvili JN: Intermolecular and Surface Forces. 3rd ed., 2011, Academic Press, New York.

(31). Bray D: Cell Movements: From Molecules to Motility. 2nd ed., 2001, Garland Science, New York.

(32). Mitchison T; Kirschner M: Dynamic instability of microtubule growth. Nature 1984, 312, 237–242. [PubMed: 6504138]

(33). Desai A; Mitchinson TJ: Microtubule polymerization dynamics. Annu. Rev. Cell Dev. Biol 1997, 13, 83–117. [PubMed: 9442869]

(34). Amos LA; Schlieper D: Microtubules and MAPs. Adv. Protein Chem 2005, 71, 257–298. [PubMed: 16230114]

(35). Shemesh A; Ginzburg A; Levi-Kalisman Y; Ringel I; Raviv U: Structure, assembly, and disassembly of tubulin single rings. Biochemistry 2018, 57, 6153–6165. [PubMed: 30247898]

(36). Himmler A; Drechsel D; Kirschner MW; Martin DW: Tau consists of a set of proteins with repeated C-terminal microtubule-binding domains and N-terminal domains. Mol. Cell Biol 1989, 9, 1381–1388. [PubMed: 2498649]

(37). Lee G; Cowan N; Kirschner MW: The primary structure and heterogeneity of Tau protein from mouse brain. Science 1988, 239, 285–288. [PubMed: 3122323]

(38). Butner KA; Kirschner MW: Tau protein binds to microtubules through a flexible array of distributed weak sites. J. Cell Biol 1991, 115, 717–730. [PubMed: 1918161]

(39). Lee G; Neve RL; Kosik KS: The microtubule binding domain of Tau protein. Neuron 1989, 2, 1615–1624. [PubMed: 2516729]

(40). Goode BL; Feinstein SC: Identification of a novel microtubule binding and assembly domain in the developmentally regulated inter-repeat region of Tau. J. Cell Biol 1994, 124, 769–782. [PubMed: 8120098]

(41). Kosik KS; Joachim CL; Selkoe DJ: Microtubule-associated protein tau (tau) is a major antigenic component of paired helical filaments in Alzheimer disease. Proc. Natl. Acad. Sci. U. S. A 1986, 83, 4044–4048. [PubMed: 2424016]

(42). Hutton M; Lendon CL; Rizzu P; Baker M; Froelich S; Houlden H; Pickering-Brown S; Chakraverty S; Isaacs A; Grover A; Hackett J; Adamson J; Lincoln S; Dickson D; Davies P; Petersen RC; Stevens M; de Graaff E; Wauters E; van Baren J; Hillebrand M; Joosse M; Kwon JM; Nowotny P; Che LK; Norton J; Morris JC; Reed LA; Trojanowski J; Basun H; Lannfelt L; Neystat M; Fahn S; Dark F; Tannenberg T; Dodd PR; Hayward N; Kwok JB; Schofield PR; Andreadis A; Snowden J; Craufurd D; Neary D; Owen F; Oostra BA; Hardy J; Goate A; van Swieten J; Mann D; Lynch T; Heutink P: Association of missense and 5'-splice-site mutations in tau with the inherited dementia FTDP-17. Nature 1998, 393, 702–705. [PubMed: 9641683]

(43). McKee AC; Cantu RC; Nowinski CJ; Hedley-Whyte ET; Gavett BE; Budson AE; Santini VE; Lee H-S; Kubilus CA; Stern RA: Chronic traumatic encephalopathy in athletes: progressive tauopathy after repetitive head injury. J. Neuropathol. Exp. Neurol 2009, 68, 709–735. [PubMed: 19535999]

(44). Jordan MA & Wilson L Microtubules as a target for anticancer drugs. Nature Reviews Cancer 2004, 4, 253–265. [PubMed: 15057285]

(45). Jordan MA; Wilson L: in Cancer Drug Discovery and Development, The Role of Microtubules in Cell Biology, Neurobiology, and Oncology, ed. Fojo T, 47–81 2008 Humana Press, New York.

(46). Miller HP; Wilson L: Preparation of Microtubule Protein and Purified Tubulin from Bovine Brain by Cycles of Assembly and Disassembly and Phosphocellulose Chromatography. Meth. Cell Biol 2010, 95, 2–15.

(47). Nogales E; Wolf SG; Khan IA; Luduena RF; Downing KH: Structure of tubulin at 6.5 Å and location of the taxol-binding site. Nature 1995, 375, 424–427. [PubMed: 7760939]

(48). Mitra A; Sept D: Taxol allosterically alters the dynamics of the tubulin dimer and increases the flexibility of microtubules. Biophys. J 2008, 95, 3252–3258. [PubMed: 18621813]

(49). Lowe J; Li H; Downing KH; Nogales E: Refined structure of alpha beta-tubulin at 3.5 A resolution. J. Mol. Biol 2001, 313, 1045–1057. [PubMed: 11700061]

(50). Stevens MJ: How shape affects microtubule and nanoparticle assembly, Science 2014, 343, 981–982. [PubMed: 24578572]

(51). Rau DC; Lee B; Parsegian VA: Measurement of the repulsive force between polyelectrolyte molecules in ionic solution: hydration forces between parallel DNA double helices. Proc. Natl. Acad. Sci. U. S. A 1984, 81, 2621–2625. [PubMed: 6585818]

(52). Chung PJ; Choi MC; Miller HP; Feinstein HE; Raviv U; Li Y; Wilson L; Feinstein SL; Safinya CR: Direct force measurements reveal that protein Tau confers short-range attractions and isoform-dependent steric stabilization to microtubules. Proc. Natl. Acad. Sci. U. S. A 2015, 112, E6416–E6425. [PubMed: 26542680]

(53). Devanand K; Selser JC: Asymptotic Behavior and Long-Range Interactions in Aqueous Solutions of Poly(ethylene oxide). Macromolecules 1991, 24, 5943–5947.

(54). Savarin P; Barbet A; Delga S; Joshi V; Hamon L; Lefevre J; Nakib S; Jean-Pascal De Bandt J-P; Moinard C; Curmi PA; Pastre D: Central role for polyamines in microtubule assembly in cells. Biochemical J 2010, 430, 151–159.

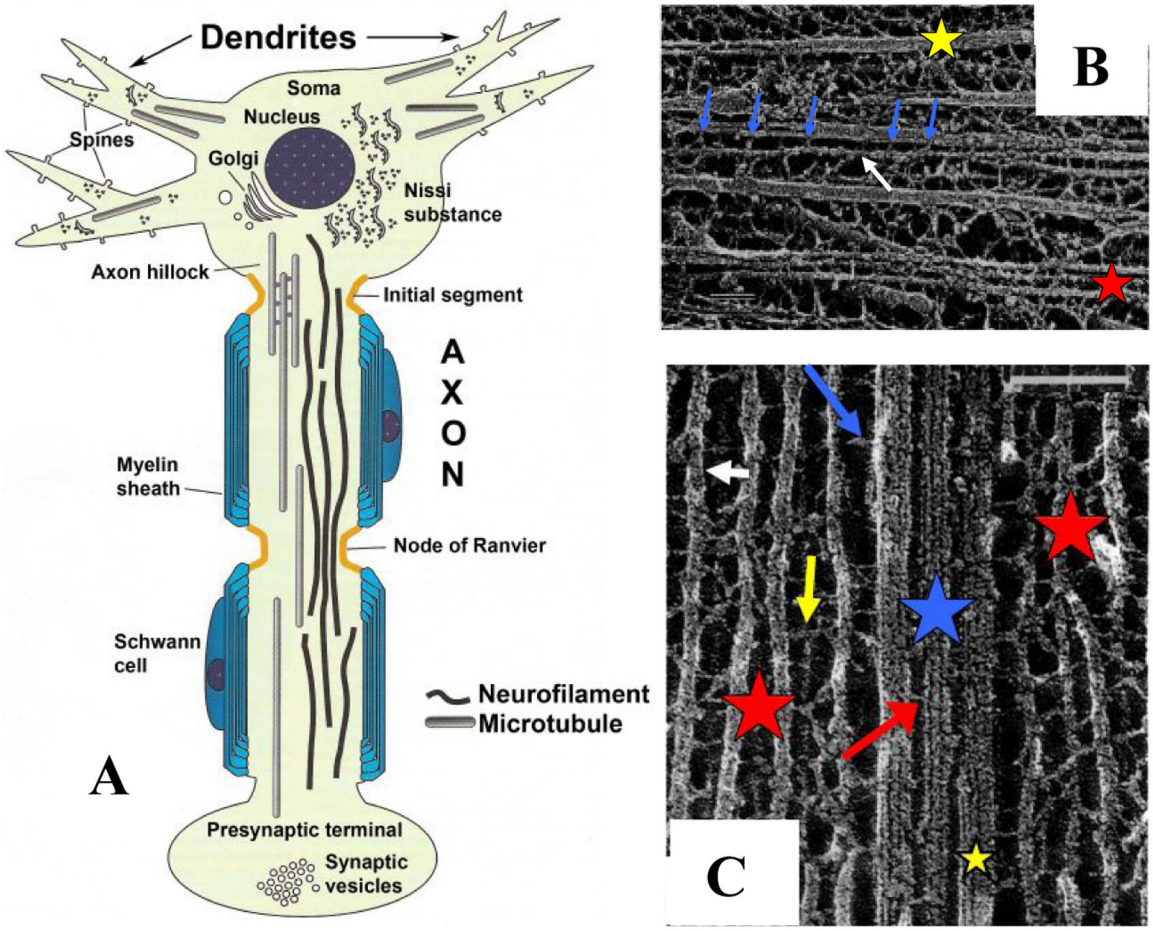

Figure. 1.

(A) Cartoon of a neuron showing elements of subcellular organization within the axon, cell body, and dendrites. Of interest to this mini-review are the heterogeneous cytoskeletal structures in distinct compartments consisting of microtubules (MTs), neurofilaments (NFs), and associated proteins. (**B, C**) Quick-freeze, deep-etch electron micrographs showing dendrite (B) and axon (C) cytoskeletons in spinal cord vertebrate neurons. In dendrites (B), MTs (one labeled by yellow star) are uniformly dispersed and NFs are either singly observed (white arrow) or in small bundles (red star). Cross-bridges between MTs and NFs are evident (microtubule-associated protein 2, MAP2, blue arrows). In axons (C), NFs (red stars) are the majority component and form oriented arrays surrounding MT bundles (blue star) or single MTs. White arrow points to NF core. Cross-bridges between NFs (NF-sidearm, yellow arrow), MTs (a microtubule-associate protein, red arrow) and MT and NF-sidearms (blue arrow) are evident. Bar = 100 nm. (A) Adapted with permission from reference 4. (B) and (C) Adapted with permission from references 5 and 6, respectively.

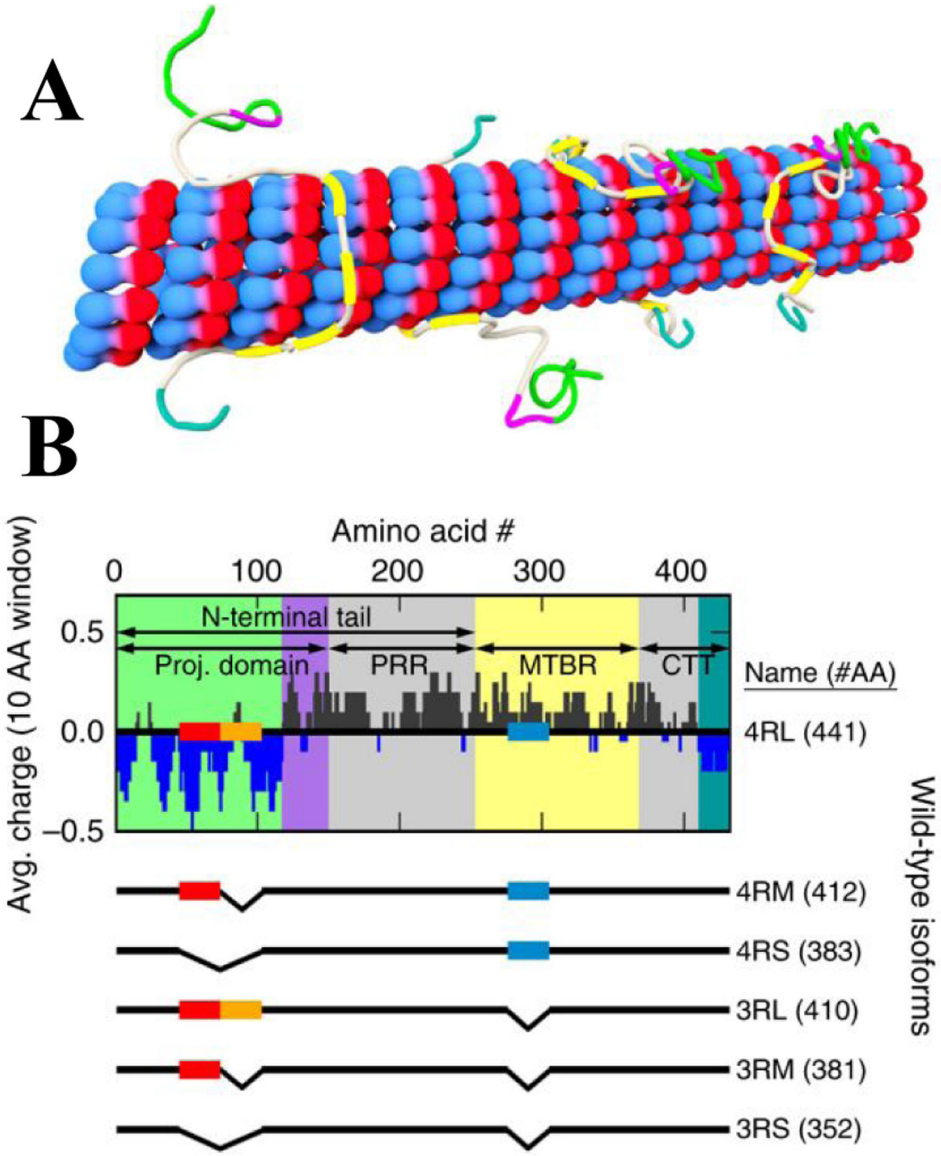

Figure. 2.

(A) Cartoon showing Tau bound to a microtubule (MT) through its MTBR (yellow) segments, with the projection domain (green/purple, the main part of the N-terminal tail) having low MT affinity. (**B**) The top depicts the charge of 4RL Tau as a function of amino acid residues. The bottom shows that alternative splicing of exons 2 (red rectangle), 3 (orange), and 10 (blue) may result in the five other wild type isoforms. Wild type Tau consists of the amino-terminal tail (NTT), which includes the projection domain (PD, green/purple background) and proline-rich region (PRR, gray), the microtubule-binding region (MTBR, yellow) and carboxyl-terminal tail (CTT). Adapted from reference 12 with permission from the Nature Publishing Group.

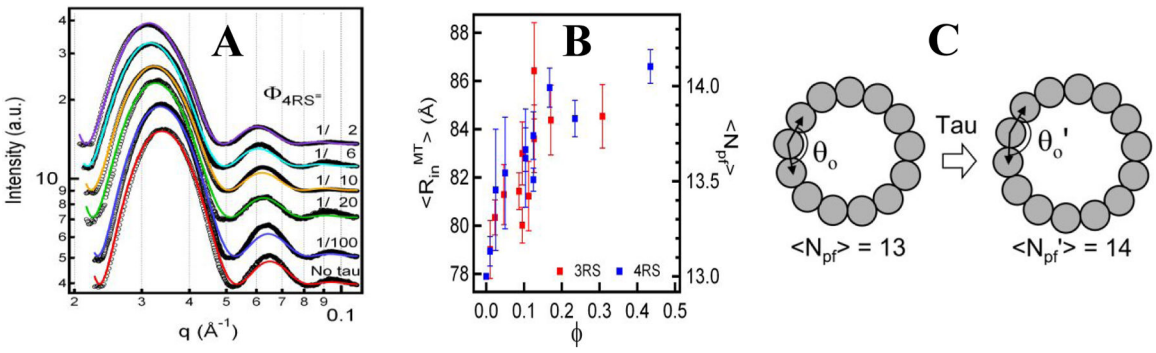

Figure. 3.

SAXS data showing that MAP Tau regulates the mean radius of MTs, or equivalently, the average protofilament number $<N_{pf}>$. **(A)** Synchrotron SAXS results of MTs with bound 4RS tau as a function of Tau to tubulin-dimer molar ratio in the reaction mixture (Φ). With increasing Tau, the SAXS profiles shift to lower q implying an increase in the MT radius. Colored lines are results of fits of the data to a model consisting of a hollow MT nanotube with the inner radius $<R_{in}>$ being the sole fitting parameter. **(B)** The average inner radius $<R_{in}>$ for two Tau isoforms (4RS and 3RS) plotted versus ϕ, the tau/tubulin-dimer molar ratio for the Tau fraction bound to the MT surface. The radial size of MTs increases as a function of increasing tau. **(C)** Schematic cross-sections of two MTs showing that with increasing Tau binding the distribution of protofilaments in MTs shifts towards MTs with larger $<N_{pf}>$, which leads to increases in $<R_{in}>$. A change in the diameter of MTs necessitates a change in the shape of tubulin dimers making up the protofilaments. Reprinted with permission from reference 23. Copyright 2009, Biophysical Society.

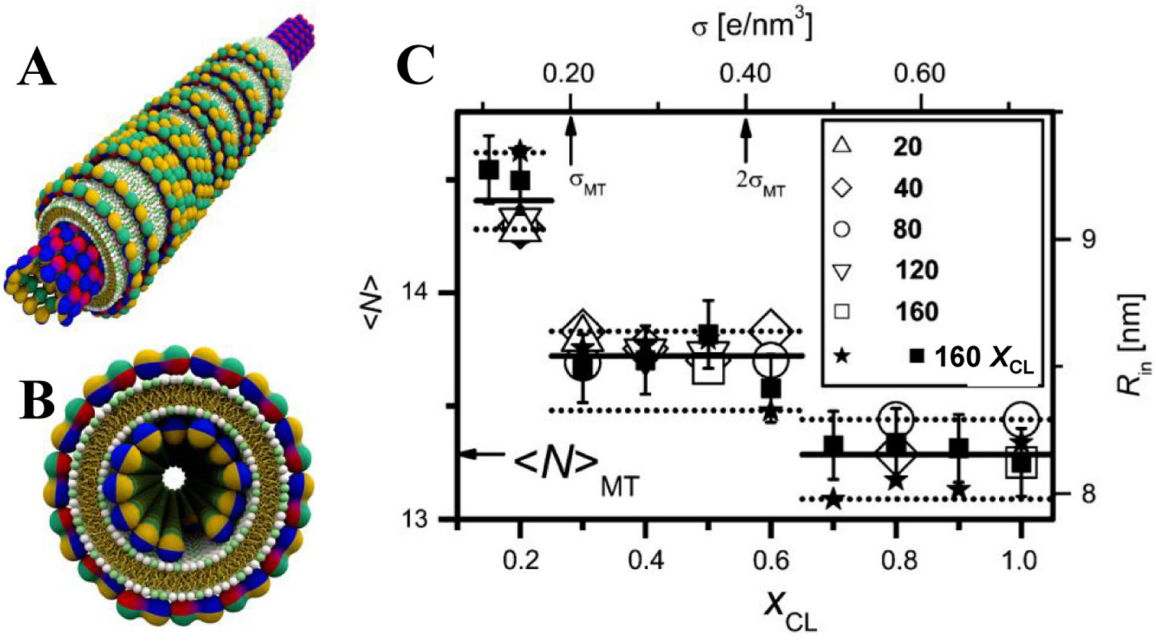

Figure 4.

(A and B) Two views of lipid protein nanotube (LPN, with cross section view in B) made of a microtubule (tubulin subunits shown as red-blue-yellow-green objects) coated by a lipid bilayer membrane containing a mixture of cationic and neutral lipids (yellow lipid tails, green cationic headgroups, and white neutral headgroups). The lipid bilayer is further coated by tubulin rings. **(C)** Plot of the average number of protofilaments (PFs) per microtubule (MT), $\langle N_{pf} \rangle$, and the inner wall radius, $\langle R_{in} \rangle$, of the MT within the LPN complex as a function of x_{CL}, the mole fraction of cationic lipids in the lipid bilayer, or the membrane charge density (σ). The symbols in the inset correspond to different charged lipid to tubulin molar ratios $R_{CL/T}$. Solid symbols, for which $R_{CL/T} = 160 \cdot x_{CL}$, correspond to a series of data points at which the total number of lipids per tubulin is kept constant and is exactly enough to coat each MT with a bilayer. The arrow indicates the $\langle N_{pf} \rangle$ value of pure MTs, $\langle N_{pf} \rangle_{MT}$ =13.3, as obtained from the fit to the MT form factor. The three solid lines indicate the mean values of $\langle N_{pf} \rangle$ at each step. The broken lines indicate the upper and lower limits of $\langle N_{pf} \rangle$ at each step. Thus, the average number of protofilaments, or equivalently, the inner radius of the microtubule, changes in a step-wise fashion as the membrane charge density is changed. Reprinted with permission from reference 25. Copyright 2007, Biophysical Society.

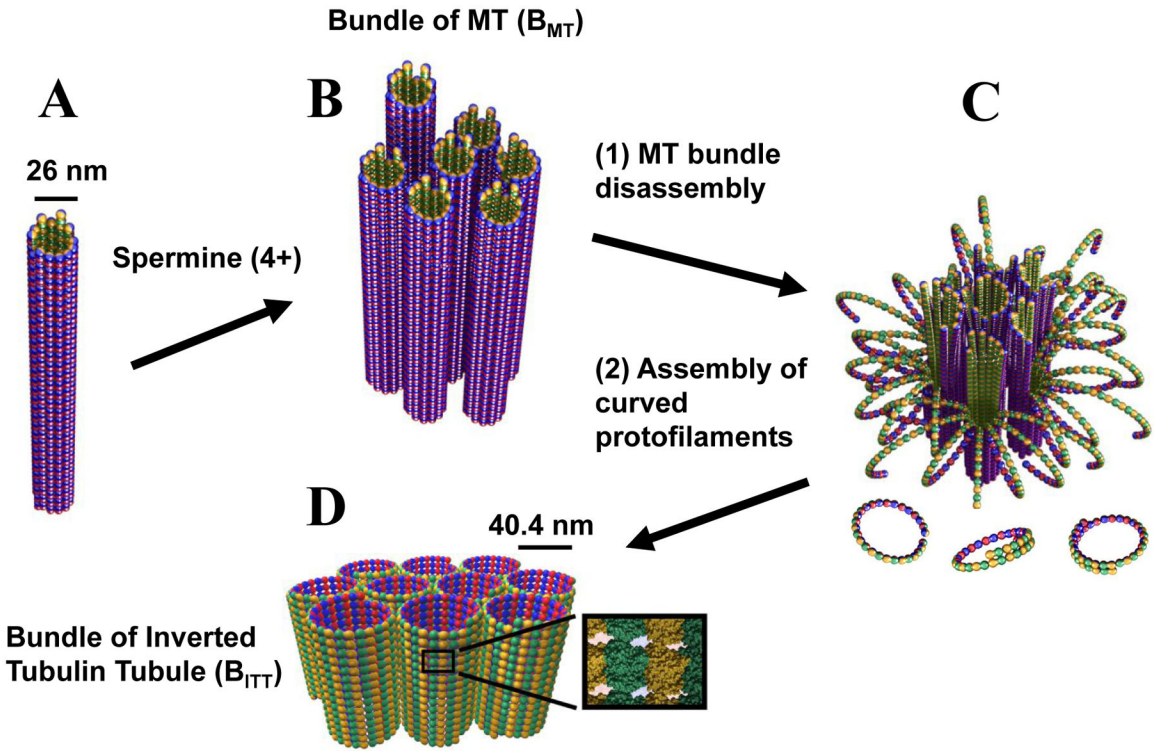

Figure. 5.

Schematic of a spermine (4+)-induced inversion process from bundles of taxol-stabilized microtubules (B_{MT}) to bundles of inverted tubulin tubules (B_{ITT}). **(A and B)** Taxol-stabilized microtubules (MTs, A) may be induced to form MT bundles above a critical concentration of spermine (4+) counterions (B_{MT}, B). The bundles result from the nonspecific electrostatic attraction between spermine coated MTs. **(C and D)** For concentrations several times larger than the critical bundling concentration a specific spermine-triggered straight-to-curved conformation transition in protofilaments, leads to MT disassembly into curved protofilaments (c-PFs) within the bundles (C). Concurrent to MT disassembly spermine counterions induce non-specific assembly of c-PFs into the B_{ITT} phase (D). Both phases are hierarchically ordered, liquid crystalline nanotubes, but the tubes are inverted: the tubulin surface, which is on the inside of the tubes in the B_{MT} phase is on the outside in the B_{ITT} phase. Adapted from reference 26 with permission from the Nature Publishing Group.

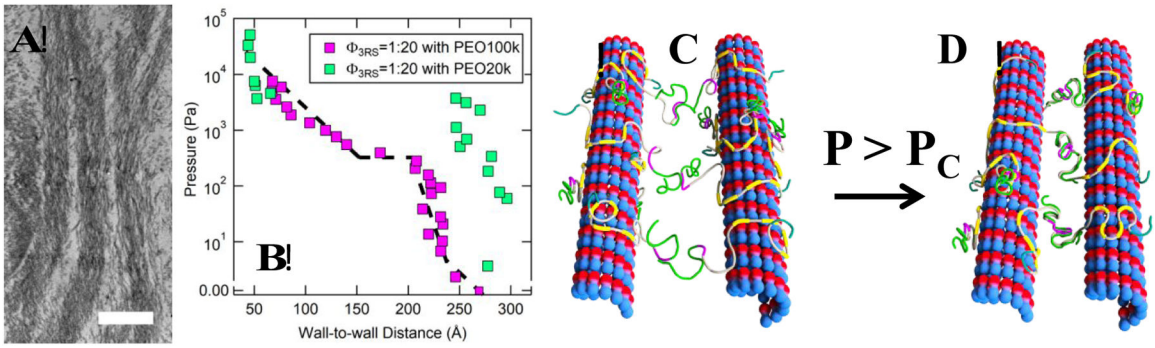

Figure 6.

Force measurements, by Synchrotron SAXS-Osmotic Pressure studies of microtubule/Tau bundles, reveal two distinct bundle states. **(A)** Plastic embedded TEM side view of microtubules (MTs) assembled with Tau (3RM-Tau, 1/20 Tau/tubulin dimer molar ratio) show finite size MT/Tau bundles. **(B):** Osmotic pressure (P) - distance ($D_{w\text{-}w}$) curves for MT/3RS-Tau bundles using either 102K-PEO (magenta) or 20K-PEO (green). For 100K-PEO with diameter ≈ 40 nm the depletant cannot penetrate the bundles and with increasing P, measurements of the MT wall-to-wall spacing ($D_{w\text{-}w}$) shows a sudden transition to a collapsed MT bundle state (≈ 5 nm decrease) at $P > P_c \approx 300$ Pa. This is indicative of a secondary energy minimum for MT bundles (magenta squares). With 20K-PEO as the polymer depletant, the transition to the collapsed bundle state is observed at higher P ≈ 5000 Pa (green squares). The discrepancy arises because the 20K-PEO depletant (diameter ≈ 15.6 nm) is smaller than the MT wall-to-wall spacing and partially penetrates the bundles giving rise to an “apparent pressure” larger than the actual applied pressure (the apparent pressure assumes the depletant does not penetrate the interior of the bundles). Above the transition the 20K-PEO depletant is expelled from the collapsed bundle and, as expected, the data for 100K-PEO and 20K-PEO overlap. **(C and D)** Cartoon of the osmotic pressure (P) induced transition from widely- spaced MT/Tau bundles (C) to a collapsed bundle state above a critical pressure (D). In the widely-spaced bundle state (C), weakly penetrating extended Tau projection domains (PDs) mediate transient charge-charge attractions between the cationic residues (purple/gray) and the anionic residues (green) of apposing PDs. The pressure induced transition to a collapsed state depicted in (D) (i.e. a secondary energy minimum at smaller spacings compared to widely-spaced bundles) corresponds to anti-parallel dimerization (i.e. ≈ full overlap) of Tau PDs occurring between the anionic section of the PD (green) and the cationic part of the PD (purple). (A, C, D) Adapted from reference 12 with permission from the Nature Publishing Group. (B) Adapted with permission from reference 28. Copyright 2018 American Chemical Society.